γ-Al_2O_3-Supported PtRu Clusters Prepared from $[Pt_2Ru_4(CO)_{18}]$: Characterization by Infrared and Extended X-ray Absorption Fine Structure Spectroscopies

Oleg S. Alexeev,[†] George W. Graham,[‡] Mordecai Shelef,[‡] Richard D. Adams,[§] and Bruce C. Gates*,[†]

Department of Chemical Engineering and Materials Science, University of California, Davis, California 95616, Ford Research Laboratory, Ford Motor Co., Dearborn, Michigan 48121, and Department of Chemistry and Biochemistry, University of South Carolina, Columbia, South Carolina 29208

Received: November 29, 2001; In Final Form: February 25, 2002

Highly dispersed γ-Al_2O_3-supported PtRu clusters were prepared by decarbonylation of molecularly adsorbed $[Pt_2Ru_4(CO)_{18}]$ in He or H_2 at temperatures in the range of 300−400 °C. Infrared (IR) and extended X-ray absorption fine structure (EXAFS) spectroscopies were used to characterize the supported species before and after removal of the CO ligands. The IR and EXAFS spectra show that most of the $[Pt_2Ru_4(CO)_{18}]$ interacted weakly through its CO ligands with the surface hydroxyl groups of γ-Al_2O_3 and could be extracted into CH_2Cl_2, but a small fraction of the $[Pt_2Ru_4(CO)_{18}]$ interacted strongly with the support and could not be extracted. The strongly bonded species, characterized by a ν_{co} band at 2063 cm^{-1}, formed as a result of nucleophilic attack of some support hydroxyl groups on carbonyl ligands, leading to the removal of these ligands as CO_2 and formation of covalent bonds between the clusters and the oxygen atoms of the support. The EXAFS data show that after decarbonylation in He or H_2 at 300−400 °C, the Pt−Ru cluster frame was changed relative to that of the supported $[Pt_2Ru_4(CO)_{18}]$. The average Pt−Pt bond distance increased from 2.66 to 2.69 Å, and the Ru−Ru distance decreased from 2.83 to 2.64 Å. The corresponding Pt−Pt and Ru−Ru coordination numbers were found to be 2.0 and 4.0, respectively, indicating that slight agglomeration of the metal took place upon decarbonylation. The EXAFS data show that the Pt−Ru interactions were largely maintained after decarbonylation, so that highly dispersed Pt−Ru structures were present on the support. From the Pt−Pt and Ru−Ru coordination numbers it follows that decarbonylated clusters incorporate, on average, less than three and six Pt and Ru atoms, respectively, being the smallest such supported bimetallic clusters of platinum-group metals yet reported.

Introduction

The wide interest in supported bimetallic catalysts is based not only on their commercial importance, as illustrated by catalysts used for naphtha reforming (Pt−Re, Pt−Sn, and Pt−Ir)[1] and auto exhaust conversion (Pt−Rh),[2] but also on the realization that catalytic activity, selectivity, and stability of a supported platinum-group metal can often be improved by the incorporation of a second metal. Extremely highly dispersed bimetallic clusters on oxide supports can be made by adsorption of molecular clusters in which the two metals are bonded to each other.[3] When a bimetallic cluster precursor incorporates a noble metal-oxophilic metal combination, the supported bimetallic particles may be extremely small (for example, less than about 10 atoms each), with the two metals present in the same clusters.[4] Removal of ligands from the adsorbed precursor leads to clusters of the noble metal inferred to be "nested" in clusters of oxides of the oxophilic metal that are strongly bonded to the oxide support and stabilize the dispersion of the noble metal.[3,4]

In supported catalysts consisting of two platinum-group metals (e.g., Pt and Ir),[5] supported bimetallic particles are typically aggregated and relatively large, incorporating tens of metal atoms or more, even when prepared from molecular cluster precursors.[6] Thus, reports of bimetallic clusters on supports that are extremely highly dispersed are limited to platinum group metal-oxophilic metal combinations, and there is a lack of evidence of such bimetallic clusters that contain just platinum-group metals.

Our goal was to prepare such highly dispersed bimetallic clusters. The precursor was $[Pt_2Ru_4(CO)_{18}]$; the choice of a platinum-containing precursor was based on the extensive applications of platinum in industrial catalysts. The combination of platinum with ruthenium was based on the availability of the precursor that incorporates two platinum-group metals bonded to each other and stabilized by small and easily removable organic ligands.

We report the preparation and characterization of γ-Al_2O_3-supported PtRu clusters by infrared (IR) and extended X-ray absorption fine structure (EXAFS) spectroscopies. The results give evidence of the interactions of the precursor $[Pt_2Ru_4(CO)_{18}]$ with γ-Al_2O_3, decarbonylation, and the formation of PtRu clusters barely larger than the Pt_2Ru_4 frame of the precursor.

Experimental Methods

Reagents and Materials. The organometallic syntheses, including sample handling, were performed with air exclusion under dry N_2 by use of vacuum-line techniques. Gases (He, N_2, and H_2 (Matheson, UHP grade)) were purified by passage through traps containing reduced Cu/Al_2O_3 and zeolite particles

* Corresponding author.
[†] University of California, Davis.
[‡] Ford Motor Co.
[§] University of South Carolina.

10.1021/jp014342i CCC: $22.00
Published on Web 04/04/2002

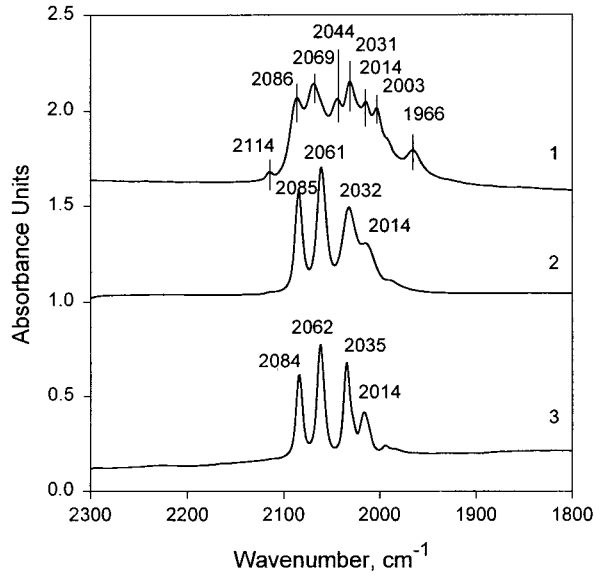

Figure 1. IR spectra in the ν_{CO} region: (1) $[Pt_2Ru_4(CO)_{18}]$ mixed with KBr powder; (2) $[Pt_2Ru_4(CO)_{18}]$ dissolved in CH_2Cl_2; (3) $[Pt_2Ru_4(CO)_{18}]$ dissolved in *n*-hexane.

to remove traces of O_2 and water, respectively. The γ-Al_2O_3 support, with a BET surface area of 100 m^2/g (determined by N_2 adsorption), was prepared as described elsewhere[7] and partially dehydroxylated under vacuum at 400 °C prior to use. The solvents (*n*-hexane and dichloromethane, Fisher, 99% purity) were dehydrated, purified by refluxing, and deoxygenated by sparging of dry N_2 prior to use.

Synthesis of Organometallic Precursors. The $[Pt_2Ru_4(CO)_{18}]$ precursor was prepared as described elsewhere.[8] $[Pt_2Ru_4(CO)_{18}]$ was separated from other reaction products on a silica gel column by elution with a CH_2Cl_2/hexane mixture and identified by IR spectroscopy in the ν_{CO} region (Figure 1), with the spectra matching those reported.[8]

Sample Preparation. The samples were prepared by slurrying of $[Pt_2Ru_4(CO)_{18}]$ in CH_2Cl_2 with γ-Al_2O_3 powder. The solvent was removed by evacuation, ensuring complete uptake of the precursor by the support. The amount of precursor was chosen to give samples containing 1.0 wt % Pt and 1.0 wt % Ru after removal of the ligands from the precursors.

IR Spectroscopy. A Bruker IFS-66v spectrometer was used to record spectra with a resolution of 4 cm^{-1}. The γ-Al_2O_3 powder was pressed into self-supporting wafers and mounted in the IR cell in a drybox. Then the interaction of $[Pt_2Ru_4(CO)_{18}]$ with the γ-Al_2O_3 surface was investigated in-situ as the sample was prepared in the IR cell. Each sample was scanned 64 times and the signal averaged.

Extraction of Surface Species. CH_2Cl_2 solvent was introduced into a Schlenk flask containing freshly prepared sample made from γ-Al_2O_3 and $[Pt_2Ru_4(CO)_{18}]$. The suspension was stirred for 30 min, and the liquid was transferred by syringe into an IR cell equipped with valves allowing isolation of the liquid. Spectra were recorded as stated above.

EXAFS Spectroscopy. EXAFS experiments were performed at X-ray beamline 2-3 at the Stanford Synchrotron Radiation Laboratory (SSRL) at the Stanford Linear Accelerator Center, Stanford, CA. The storage ring energy was 3 GeV and the ring current 60−100 mA. EXAFS spectroscopy was used to characterize the surface species formed after contacting the γ-Al_2O_3 with a CH_2Cl_2 solution of $[Pt_2Ru_4(CO)_{18}]$ as well as after decarbonylation the surface species in He or H_2. The sample handling was as described elsewhere.[7,9]

The EXAFS data were collected in transmission mode after the cell had been cooled to nearly liquid nitrogen temperature. The data were collected with a Si(220) double crystal monochromator that was detuned by 20% to minimize effects of higher harmonics in the X-ray beam. The samples were scanned at energies near the Pt L_{III} (11564 eV) and Ru *K* (22117 eV) absorption edges.

EXAFS Reference Data and Analysis

The EXAFS data were analyzed with experimentally and theoretically determined reference files, the former obtained from EXAFS data for materials of known structure. The Pt−Pt, Pt−$O_{support}$, Ru−$O_{support}$, and Ru−CO interactions were analyzed with phase shifts and backscattering amplitudes obtained from EXAFS data for Pt foil, $Na_2Pt(OH)_6$, RuO_2, and $[Ru_3(CO)_{12}]$, respectively. As the phase shift and backscattering amplitude are to a good approximation transferable between next-near neighbors in the periodic table, the Ir−C and Ir−O* phase shifts and backscattering amplitudes extracted from EXAFS data characterizing crystalline $[Ir_4(CO)_{12}]$ were used to analyze the Pt−CO (Pt−C and Pt−O*) interactions.[10] The Ru−Ru, Pt−Ru, and Ru−Pt interactions were calculated on the basis of the crystallographic data reported for metallic Ru and $[PtRu_2(CO)_8(dppe)]$ (dppe is 1,2-bis(diphenylphosphino)ethane) by use of the FEFF software.[11] The EXAFS parameters were extracted from the raw data with the XDAP software.[12] The methods used to extract the EXAFS function from the raw data are essentially the same as those reported.[7] Data representing each sample are the average of six scans. The analysis was carried out as follows.

The raw EXAFS data obtained at Pt L_{III} edge were analyzed with a maximum of 24 free parameters over the ranges $3.20 < k < 15.0$ Å^{-1} (*k* is the wave vector) and $0.0 < r < 4.0$ Å (*r* is the distance from the absorber atom, in this case Pt). The statistically justified number of free parameters, *n*, was about 31, as estimated from the Nyquist theorem,[13,14] $n = (2\Delta k \Delta r/\pi) + 1$, where Δk and Δr, respectively, are the *k* and *r* ranges used to fit the data.

The raw EXAFS data obtained at the Ru *K* edge were analyzed with a maximum of 24 free parameters over the ranges $4.26 < k < 15.50$ Å^{-1} and $0.0 < r < 4.0$ Å. The statistically justified number of free parameters, estimated as described above, was about 29.

The data analysis was done with a difference file technique.[15,16] The approach used to analyze the data at the Pt L_{III} and at Ru *K* edges was similar to that described.[17] The reliable parameters for the high-Z (Pt, Ru) and low-*Z* contributions ($O_{support}$, CO) were determined by multiple-shell fitting in *r* space and in *k* space with application of k^1 and k^3 weightings.[18]

Results

IR Evidence of Interaction of $[Pt_2Ru_4(CO)_{18}]$ with γ-Al_2O_3. IR spectra characterizing the ν_{OH} region of γ-Al_2O_3 before and after interaction with a CH_2Cl_2 solution of $[Pt_2Ru_4(CO)_{18}]$ are shown in Figure 2. The spectrum representing bare γ-Al_2O_3 after treatment under vacuum at 400 °C includes bands at 3794, 3772, 3730, and 3671 cm^{-1}, assigned to several types of isolated hydroxyl groups[19] (Figure 2, spectrum 1). The broad band at 3581 cm^{-1} represents hydrogen-bonded OH groups.[19]

After contacting of the γ-Al_2O_3 wafer with the CH_2Cl_2 solution of $[Pt_2Ru_4(CO)_{18}]$ followed by the solvent removal by evacuation into a trap cooled to liquid nitrogen temperature, the intensity of the band associated with hydrogen-bonded hydroxyl groups increased relative to that characteristic of the

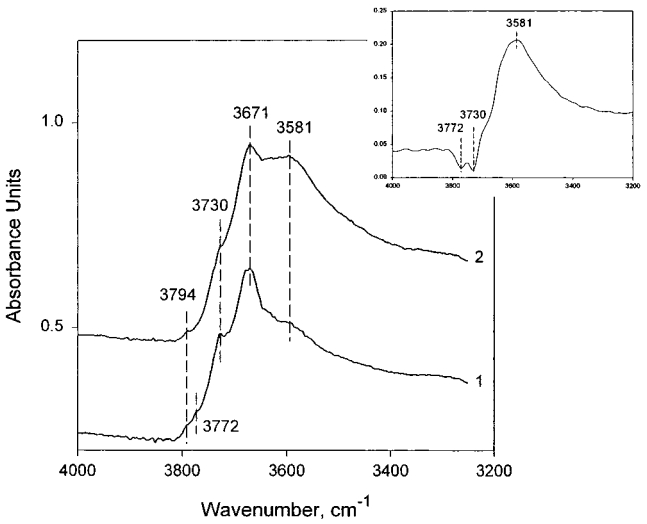

Figure 2. IR spectra in the ν_{OH} region characterizing the interaction of $[Pt_2Ru_4(CO)_{18}]$ with the γ-Al_2O_3 surface: (1) Bare γ-Al_2O_3 treated under vacuum at 400 °C; (2) sample formed by contacting of γ-Al_2O_3 with $[Pt_2Ru_4(CO)_{18}]$ in CH_2Cl_2 and followed by removal of the solvent by condensation in a trap held at liquid nitrogen temperature. The inset at the upper right demonstrates the difference spectrum obtained by subtracting spectrum 1 from spectrum 2.

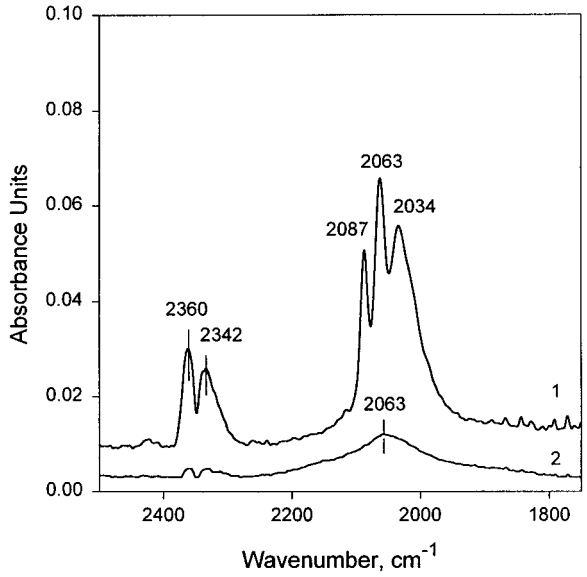

Figure 3. IR spectra in the ν_{CO} region: (1) Sample formed by contacting of γ-Al_2O_3 with $[Pt_2Ru_4(CO)_{18}]$ in CH_2Cl_2 and removal of the solvent by condensation in a trap cooled to liquid nitrogen temperature; (2) sample after extraction of supported species with CH_2Cl_2.

cluster-free γ-Al_2O_3, and the intensities of bands representing isolated hydroxyl groups, at 3772 and 3730 cm^{-1}, decreased (Figure 2, spectrum 2 and inset). New bands associated with ν_{co} of the precursor carbonyl ligands arose at 2087, 2063, and 2034 cm^{-1} (Figure 3, spectrum 1) along with bands at 2360 and 2342 cm^{-1}, assigned to gas-phase CO_2.[20] After complete removal of the solvent by evacuation at 25 °C, the spectrum was slightly changed in the ν_{co} region, and bands associated with carbonyl ligands were observed at 2140, 2074, 2041, and 2008 cm^{-1} (Figure 4). All ν_{CO} bands were removed by treatment in He or H_2 at 300 °C.

IR Evidence of Extraction of Adsorbed Clusters. Surface species formed by adsorption of $[Pt_2Ru_4(CO)_{18}]$ were extracted from γ-Al_2O_3 by CH_2Cl_2 at room temperature. The ν_{co} bands at 2140, 2074, 2041, 2008 cm^{-1}, assigned to supported $[Pt_2Ru_4(CO)_{18}]$, disappeared, and the extract solution was characterized by ν_{co} bands at 2085, 2061, 2032, and 2014 cm^{-1}; these are virtually the same as those observed for $[Pt_2Ru_4(CO)_{18}]$ dissolved in CH_2Cl_2 (Figure 1, spectrum 2). This result suggests the molecular adsorption of the precursor on γ-Al_2O_3.

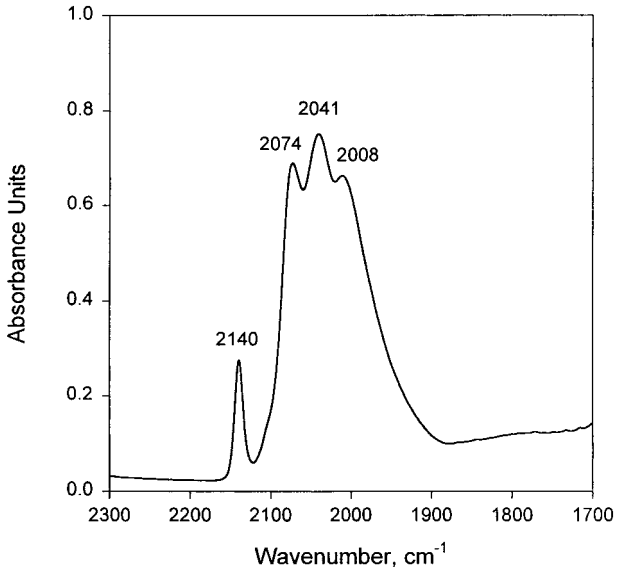

Figure 4. IR spectra in the ν_{CO} region characterizing sample formed by contacting of γ-Al_2O_3 with $[Pt_2Ru_4(CO)_{18}]$ in CH_2Cl_2 and removal of the solvent by evacuation at 25 °C.

TABLE 1: Summary of EXAFS Data Characterizing γ-Al_2O_3-supported $[Pt_2Ru_4(CO)_{18}]$[a]

edge	shell	N	R (Å)	$10^3 \cdot \Delta\sigma^2$ (Å^2)	ΔE_0 (eV)
Pt L_{III}	Pt−Pt	1.0 ± 0.1	2.66 ± 0.01	0.3 ± 0.2	3.0 ± 0.7
	Pt−Ru	3.0 ± 0.1	2.77 ± 0.01	8.8 ± 0.2	−9.0 ± 0.1
	Pt−CO				
	Pt−C	1.4 ± 0.1	1.83 ± 0.01	4.6 ± 0.6	−5.4 ± 0.3
	Pt−O*	1.5 ± 0.1	2.92 ± 0.01	−1.4 ± 0.1	3.9 ± 0.1
	$Pt-O_{support}$				
	$Pt-O_s$	1.2 ± 0.1	2.26 ± 0.01	10.0 ± 0.8	−18.2 ± 0.5
	$Pt-O_l$	3.4 ± 0.1	3.20 ± 0.01	5.3 ± 0.5	−8.1 ± 0.2
Ru K	Ru−Ru	1.0 ± 0.1	2.83 ± 0.01	2.1 ± 0.2	9.8 ± 0.7
	Ru−Pt	1.6 ± 0.1	2.77 ± 0.01	8.8 ± 0.8	2.2 ± 1.1
	Ru−CO				
	Ru−C	3.8 ± 0.1	1.94 ± 0.01	2.4 ± 0.1	1.0 ± 0.2
	Ru−O*	3.9 ± 0.1	3.05 ± 0.01	0.1 ± 0.0	−2.0 ± 0.2
	$Ru-O_{support}$				
	$Ru-O_s$	3.0 ± 0.1	2.13 ± 0.01	10.0 ± 0.4	1.2 ± 0.5
	$Ru-O_l$	1.5 ± 0.1	3.24 ± 0.01	−3.6 ± 0.2	3.3 ± 0.4

[a] Notation: N, coordination number; R, distance between absorber and backscatterer atoms; $\Delta\sigma^2$, Debye−Waller factor; ΔE_0, inner potential correction; the subscripts s and l refer to short and long, respectively.

However, a small portion of the supported species could not be extracted from the γ-Al_2O_3, as indicated by a weak, broad band centered at 2063 cm^{-1} (Figure 3, spectrum 2).

EXAFS Data Characterizing Surface Species Formed after Interaction of $[Pt_2Ru_4(CO)_{18}]$ with γ-Al_2O_3 and Subsequent Decarbonylation. The EXAFS results characterizing γ-Al_2O_3-supported $[Pt_2Ru_4(CO)_{18}]$ at the Pt L_{III} and Ru K edges are summarized in Table 1. A comparison of X-ray diffraction (XRD) and EXAFS data characterizing crystalline and supported $[Pt_2Ru_4(CO)_{18}]$ is included in Table 2. The structure parameters determined from the EXAFS data characterizing the surface species formed by decarbonylation of γ-Al_2O_3-supported $[Pt_2Ru_4(CO)_{18}]$ in He or in H_2 at various temperatures are shown in Tables 3 and 4 for the Pt L_{III} and Ru K edges, respectively. The error bounds in the parameters reported in Tables 1, 3, and

TABLE 2: Comparison XRD and EXAFS Data Characterizing Crystalline and γ-Al_2O_3-Supported $[Pt_2Ru_4(CO)_{18}]$[a]

	XRD data characterizing crystalline $[Pt_2Ru_4(CO)_{18}]$[8]		EXAFS data characterizing $[Pt_2Ru_4(CO)_{18}]/\gamma$-$Al_2O_3$	
shell	*R* (Å)	*N*	*R* (Å)	*N*
Pt−Pt	2.67	1.0	2.66	1.0
Pt−Ru	2.78	3.0	2.77	3.0
Pt−CO				
Pt−C	1.83	1.0	1.83	1.4
Pt−O*	2.97	1.0	2.92	1.5
Ru−Ru	2.85	1.0	2.83	1.0
Ru−Pt	2.78	1.5	2.77	1.6
Ru−CO				
Ru−C	1.93	4.0	1.94	3.8
Ru−O*	3.07	4.0	3.05	3.9

[a] Notation: XRD, X-ray diffraction; *R*, interatomic distance; *N*, first-shell coordination number.

4 represent precisions determined from statistical analysis of the data with the XDAP software,[12] not accuracies. Estimated accuracies are as follows: coordination number (*N*), ±20%; distance (*R*), ±1%; Debye−Waller factor ($\Delta\sigma^2$), ±30%; inner potential correction (ΔE_0), ±10%. Reliability of the data obtained at each edge and characterizing Pt−Ru interactions was evaluated on the basis of constraints reported earlier[21] and applied to analysis of bimetallic samples.[4]

Discussion

Evidence of Molecular Adsorption of $[Pt_2Ru_4(CO)_{18}]$ on γ-Al_2O_3. When $[Pt_2Ru_4(CO)_{18}]$ in CH_2Cl_2 was brought in contact with γ-Al_2O_3 followed by removal of the majority of the solvent by condensation in a trap cooled to liquid nitrogen temperature, ν_{co} bands appeared at 2087, 2063, and 2034 cm^{-1} (Figure 3, spectrum 1). Typically, the ν_{co} bands characterizing metal carbonyl clusters in the solid state (or those supported on a solid) differ substantially from those characterizing the same clusters in solution, in part as a consequence of the variety of vibrations that are allowed by the symmetries of the molecule in various environments (Figure 1).[22] The observation that the spectrum resembles that of $[Pt_2Ru_4(CO)_{18}]$ dissolved in CH_2Cl_2 (Figure 1, spectrum 2) is consistent with the suggestion that the bands at 2087, 2063, and 2034 cm^{-1} characterize molecular $[Pt_2Ru_4(CO)_{18}]$ on the γ-Al_2O_3 in a CH_2Cl_2 environment. The bands observed at 2988 and 3060 cm^{-1} (spectrum not shown) match the ν_{CH} of CH_2Cl_2, indicating that some solvent remained on the γ-Al_2O_3 surface at this step of the sample preparation. Thus, we infer that the reactivity of $[Pt_2Ru_4(CO)_{18}]$ with γ-Al_2O_3 in the presence of adsorbed solvent was low enough to prevent strong cluster−surface interactions. Similarly, tetrahydrofuran has been shown to minimize the interaction of $[Mn(CO)_5]^-$ with MgO.[23]

When the solvent had been completely removed by evacuation, however, the spectrum of the metal carbonyl species on γ-Al_2O_3 was characterized by ν_{co} bands at 2140, 2074, 2041, and 2008 cm^{-1} (Figure 4). This spectrum does not closely resemble that of $[Pt_2Ru_4(CO)_{18}]$ in solution or in the solid state (Figure 1), but some of the ν_{co} bands are close in frequency to bands characterizing solid $[Pt_2Ru_4(CO)_{18}]$. For example, the band at 2074 cm^{-1} characterizing the γ-Al_2O_3-supported species (Figure 4) is suggested to represent a superposition of the two bands observed at 2086 and 2069 cm^{-1} in the spectrum of solid $[Pt_2Ru_4(CO)_{18}]$ (Figure 1, spectrum 1), and the band at 2008 cm^{-1} may represent a superposition of the 2014- and 2003-cm^{-1} bands that are also evident in spectrum 1 of Figure 1. The third band characterizing the γ-Al_2O_3-supported species (at 2041 cm^{-1}) is close in frequency to the 2044-cm^{-1} band of solid $[Pt_2Ru_4(CO)_{18}]$.

Thus, the ν_{co} data suggest the presence of molecular $[Pt_2Ru_4(CO)_{18}]$ on the surface of γ-Al_2O_3 from which the solvent had been removed, but they are not regarded as conclusive evidence of its presence. To clarify the identification, the sample was brought in contact with CH_2Cl_2, and the IR spectrum of the extract solution was recorded and found to be indistinguishable from that of $[Pt_2Ru_4(CO)_{18}]$ in CH_2Cl_2 (Figure 1, spectrum 2), signifying that the cluster precursor had been extracted intact from the γ-Al_2O_3.

The EXAFS data (Tables 1 and 2) provide further strong evidence of molecular adsorption of $[Pt_2Ru_4(CO)_{18}]$ on γ-Al_2O_3. Crystallographic data[8] reported for $[Pt_2Ru_4(CO)_{18}]$ (Table 2) show that the cluster core consists of two Pt atoms bonded to

TABLE 3: Summary of EXAFS Data at the Pt L_{III} Edge Characterizing the Surface Species Formed by Decarbonylation of γ-Al_2O_3-supported $[Pt_2Ru_4(CO)_{18}]$ in He or in H_2 at Various Temperatures[a]

treatment gas/temp. (°C)	Pt−Pt contribution				Pt−Ru contribution				Pt−$O_{support}$ (Pt−O_s[b] and Pt−O_l[c]) contributions			
	N	*R* (Å)	$10^3 \times \Delta\sigma^2$ (Å^2)	ΔE_0 (eV)	*N*	*R* (Å)	$10^3 \times \Delta\sigma^2$ (Å^2)	ΔE_0 (eV)	*N*	*R* (Å)	$10^3 \times \Delta\sigma^2$ (Å^2)	ΔE_0 (eV)
H_2/300	2.0 ± 0.1	2.69 ± 0.01	5.1 ± 0.7	4.6 ± 0.6	3.0 ± 0.1	2.68 ± 0.01	5.6 ± 0.2	0.9 ± 0.2	1.4 ± 0.1[b]	2.16 ± 0.01	10.0 ± 1.2	−8.6± 0.7
									0.7 ± 0.1[c]	2.59 ± 0.01	−8.3 ± 0.2	−0.5 ± 0.9
H_2/400	2.0 ± 0.1	2.69 ± 0.01	4.7 ± 0.7	0.3 ± 0.6	3.0 ± 0.1	2.68 ± 0.01	6.1 ± 0.3	0.9 ± 0.2	1.4 ± 0.1[b]	2.15 ± 0.01	10.0 ± 1.6	−7.9 ± 0.9
									0.8 ± 0.1[c]	2.59 ± 0.01	−8.2 ± 0.2	2.6 ± 1.0
He/300	1.9 ± 0.2	2.69 ± 0.01	4.6 ± 0.7	4.7 ± 0.9	2.8 ± 0.1	2.68 ± 0.01	5.4 ± 0.3	0.8 ± 0.3	1.3 ± 0.1[b]	2.15 ± 0.01	10.0 ± 1.9	−7.9 ± 1.3
									0.6 ± 0.1[c]	2.58 ± 0.01	−7.7 ± 0.4	2.7 ± 1.8
He/400	1.9 ± 0.1	2.69 ± 0.01	4.0 ± 0.5	4.7 ± 0.7	2.8 ± 0.1	2.68 ± 0.01	5.0 ± 0.2	0.9 ± 0.2	1.3 ± 0.1[b]	2.15 ± 0.01	10.0 ± 1.5	−7.0 ± 1.2
									0.7 ± 0.1[c]	2.59 ± 0.01	−6.5 ± 0.4	0.7 ± 1.2

[a] Notation as in Table 1.

TABLE 4: Summary of EXAFS Data at the Ru *K* Edge Characterizing the Surface Species Formed by Decarbonylation of γ-Al_2O_3-Supported $[Pt_2Ru_4(CO)_{18}]$ in He or in H_2 at Various Temperatures[a]

treatment gas/temp. (°C)	Ru−Ru contribution				Ru−Pt contribution				Ru−$O_{support}$ (Ru−O_s) contribution			
	N	*R* (Å)	$10^3 \times \Delta\sigma^2$ (Å^2)	ΔE_0 (eV)	*N*	*R* (Å)	$10^3 \times \Delta\sigma^2$ (Å^2)	ΔE_0 (eV)	*N*	*R* (Å)	$10^3 \times \Delta\sigma^2$ (Å^2)	ΔE_0 (eV)
H_2/300	4.1 ± 0.1	2.64 ± 0.01	3.6 ± 0.1	4.2 ± 0.1	1.5 ± 0.1	2.68 ± 0.01	5.6 ± 0.4	2.5 ± 0.7	0.3 ± 0.1	2.09 ± 0.02	10.0 ± 4.4	−0.4± 2.2
H_2/400	4.2 ± 0.1	2.64 ± 0.01	3.6 ± 0.1	0.9 ± 0.1	1.5 ± 0.1	2.68 ± 0.01	6.1 ± 0.5	−2.5 ± 0.9	0.3 ± 0.1	2.13 ± 0.03	10.0 ± 6.1	−14.1 ± 2.6
He/300	3.2 ± 0.1	2.64 ± 0.01	3.3 ± 0.2	2.2 ± 0.2	1.5 ± 0.1	2.68 ± 0.01	5.8 ± 0.6	2.5 ± 1.4	0.8 ± 0.1	2.19 ± 0.01	10.0 ± 3.4	−13.7 ± 1.1
He/400	3.9 ± 0.1	2.64 ± 0.01	3.4 ± 0.1	1.4 ± 0.1	1.5 ± 0.1	2.68 ± 0.01	5.1 ± 0.2	−2.4 ± 0.4	0.8 ± 0.1	2.13 ± 0.01	10.0 ± 0.9	−10.3 ± 0.4

[a] Notation as in Table 1.

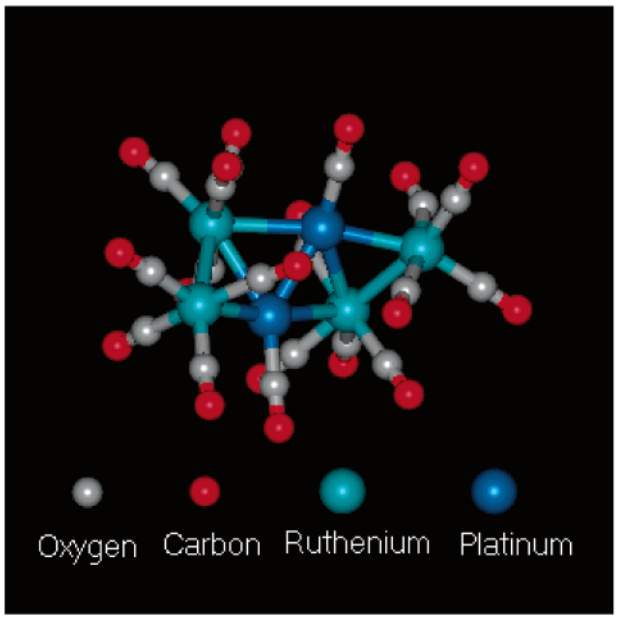

Figure 5. Structure of crystalline $[Pt_2Ru_4(CO)_{18}]$ determined on the basis of XRD data.[8]

each other at an average distance of 2.67 Å, with each of these Pt atoms being bonded to three Ru atoms at an average distance of 2.78 Å (Figure 5). The cluster core is stabilized by 18 terminal CO ligands, two of them bonded to Pt atoms with average Pt−C and Pt−O* distances (O* is carbonyl oxygen) of 1.83 and 2.97 Å, respectively; the remainder of the CO ligands are bonded to Ru atoms, with average Ru−C and Ru−O* distances of 1.93 and 3.07 Å, respectively.

The Pt L_{III} edge EXAFS data (Tables 1 and 2) characterizing the surface species formed after contacting of $[Pt_2Ru_4(CO)_{18}]$ with γ-Al_2O_3 in CH_2Cl_2 followed by removal of the solvent by evacuation indicate that each Pt atom was in close proximity to at least one Pt atom and three Ru atoms, at average distances of 2.66 and 2.77 Å, respectively. Pt−C and Pt−O* contributions indicating the presence of the terminal carbonyl ligands in the immediate neighborhood of Pt atoms were also observed, with average coordination numbers of 1.4 and 1.5 at average distances of 1.83 and 2.92 Å, respectively.

The EXAFS data collected at the Ru *K* edge complement those acquired at Pt L_{III} edge, showing that each Ru atom on average was surrounded by one Ru atom and about 1.6 Pt atoms at average distances of 2.83 and 2.77 Å, respectively. About four carbonyl groups with characteristic Ru−C and Ru−O* distances of 1.94 and 3.05 Å, respectively, were also observed in the immediate neighborhood of Ru (Table 1).

Thus, the EXAFS results at both the Pt L_{III} and Ru *K* edges characterizing the surface species formed from $[Pt_2Ru_4(CO)_{18}]$ and γ-Al_2O_3 after removal of the solvent match, within the expected experimental uncertainty, the XRD data representing solid $[Pt_2Ru_4(CO)_{18}]$.[8] The fact that all the coordination numbers and bond distances characterizing the Pt−Pt, Pt−Ru, and Ru−Ru interactions in the γ-Al_2O_3-supported $[Pt_2Ru_4(CO)_{18}]$ were almost the same as those characterizing crystalline $[Pt_2Ru_4(CO)_{18}]$ (Table 2) implies only weak cluster−support interactions that were predominantly weak enough to maintain the metal cluster frame and the Pt−Ru bonds in the adsorbed species. The EXAFS results indicating that only the Pt−O* and Ru−O* distances determined for our supported clusters are (slightly) different from those in crystalline $[Pt_2Ru_4(CO)_{18}]$ imply some distortion of the ligand environment of $[Pt_2Ru_4(CO)_{18}]$ upon interaction with the support. Similar results were reported[7] for the interaction of $[Ir_4(CO)_{12}]$ with γ-Al_2O_3.

In contrast, results of density functional theory indicate that when interactions between $[Ru_{12}Cu_4C_2(CO)_{32}Cl_2]^{2-}$ and the surface of silica were strong, the structure of the cluster frame was significantly altered, with the Cu−Cu bond distances and angles changed with respect to those in the original cluster.[24,25] The variability of surface structures formed from metal carbonyl clusters and oxide supports is broadly indicated by the literature. Some data point to clusters adsorbed intact on supports,[26] but some cluster cores are broken up upon adsorption, for example those of FeRu bimetallic clusters of various composition on Al_2O_3.[27] One would assume that the structure of the surface species depends not only on the nature of the cluster, but also on the chemistry of the support,[26] including its degree of hydroxylation,[27,28] and the strength of cluster−support interaction. Even the choice of the solvent used in the preparation may be important.[28,29] For example, Al_2O_3-supported $[RuCo_2(CO)_{11}]$ undergoes rapid disproportionation to yield $[RuCo_3(CO)_{12}]$ when the solvent is THF but not when the solvent is *n*-pentane.[29]

Nature of Cluster−Support Interactions. The chemistry of metal carbonyls on γ-Al_2O_3 is complex and typically interpreted on the basis of the acid-base character of the support. Various interactions of carbonyl ligands with the surface have been suggested. These include a weak hydrogen-bonding interaction of the coordinated CO with surface hydroxyl groups, the interaction of the coordinated CO with Lewis acid sites (Al^{3+} ions) at the surface, and reactions involving basic surface sites (such as O^{2-} or OH^-) and the coordinated CO ligands resulting in conversion of these ligands.[30] Our IR results demonstrate that the carbonyl ligands of $[Pt_2Ru_4(CO)_{18}]$ indeed play a role in the initial anchoring of the clusters to the oxide surface. We did not observe bands in the range of 1550−1660 cm^{-1}, which would indicate coordination of metal-bound CO groups through their oxygen atoms to Al^{3+} ions (as was observed for γ-Al_2O_3-supported $[Mo(CO)_6]$ and $[(C_5H_5)_3Nb_3(CO)_7]$[30]). However, the IR data (Figure 2) give clear evidence of an increase in the relative intensities of bands indicating hydrogen-bonded OH groups resulting from adsorption of $[Pt_2Ru_4(CO)_{18}]$ and suggest that a majority of the clusters were weakly adsorbed on γ-Al_2O_3 through hydrogen bonding of the surface OH groups with carbonyl ligands. Similarly, hydrogen-bonded OH groups were observed by IR spectroscopy to result from the adsorption of $[Ni(CO)_4]$ on MgO; the data were interpreted as an indication of weak hydrogen-bonding interactions between the nickel carbonyls and OH groups.[31]

Evidence of Strong Interactions between $[Pt_2Ru_4(CO)_{18}]$ and γ-Al_2O_3. The fact that a small fraction of the supported metal carbonyl species could not be extracted from γ-Al_2O_3 is consistent with the inference that some of the clusters were strongly bonded to the support. IR data showing that a decline in intensity of the ν_{OH} bands at 3772 and 3730 cm^{-1} (assigned to isolated OH groups of the support) as a result of adsorption of $[Pt_2Ru_4(CO)_{18}]$ (Figure 2), combined with the observation of CO_2 evolution (Figure 3, spectrum 1), imply that some of the surface hydroxyl groups interacted strongly with the carbonyl ligands. We infer that the interaction involved a nucleophilic attack; according to theoretical calculations,[32] nucleophilic displacement of carbonyl ligands is the most energetically favored among the various interactions suggested for γ-Al_2O_3-supported metal carbonyls. Such a surface reaction could proceed via simple decarbonylation as a result of the cleavage of CO ligands of the metal carbonyl and formation of metal−$O_{support}$ bonds,[32] or it could be similar to the reaction observed

for $[Ru_3(CO)_{12}]$ with aqueous base (KOH), which results in the formation of $[HRu_3(CO)_{11}]^-$ and evolution of CO_2.[33] The latter type of reaction was demonstrated, for example, for the interaction of $[Fe_3(CO)_{12}]$ with partially dehydroxylated γ-Al_2O_3, resulting in the formation of supported $[HFe_3(CO)_{11}]^-$ and CO_2.[30]

It is likely that these two types of reactions compete with each other, complicating the surface chemistry. Typically, the formation of anionic metal carbonyl clusters manifests itself by the shifting of terminal ν_{CO} bands to lower frequencies.[26] Our IR data indicate that the spectrum characterizing the species strongly bonded to γ-Al_2O_3 was substantially different from that observed for the weakly adsorbed $[Pt_2Ru_4(CO)_{18}]$. The former is characterized by a weak, single broad band at 2063 cm^{-1} (Figure 3, spectrum 2), which is in the same frequency range as the ν_{co} observed for the neutral $[Pt_2Ru_4(CO)_{18}]$. Thus, notwithstanding the fact that the IR data indicate the presence of CO_2 in the gas phase, the data are not conclusive regarding the formation of any anions derived from $[Pt_2Ru_4(CO)_{18}]$. We suggest that the surface species that remained on the surface after extraction were simply fragments of $[Pt_2Ru_4(CO)_{18}]$ that had been decarbonylated to various degrees and covalently bonded to the γ-Al_2O_3 surface at oxygen atoms.

The EXAFS data characterizing the γ-Al_2O_3-supported $[Pt_2Ru_4(CO)_{18}]$ (Table 1) support this suggestion by indicating $Pt-O_{support}$ and $Ru-O_{support}$ contributions at both relatively short distances that correspond to metal−oxygen bonding distances (as well as longer distances). The EXAFS data indicate $Pt-O_s$ contributions (the subscript s refers to short) at a distance of 2.26 Å (with a coordination number of 1.2) and $Ru-O_s$ contributions at a distance of 2.13 Å (with an average coordination number of 3.0). These distances are typical of the bonding of platinum-group metals in highly dispersed clusters with surface oxygen atoms of oxide supports.[34] Consistent with this conclusion, quantum chemical calculations show that ligand-free Ir_4 clusters on zeolite NaX are characterized by about the same metal−oxygen distance,[35] as are copper atoms in copper clusters on silica.[36]

Although the EXAFS data show that some metal atoms in the supported clusters are within a bonding distance of oxygen atoms of the support, we emphasize that not all of them are so close to the surface, because many are bonded to CO ligands. The longer (nonbonding) metal−oxygen distances are evidenced by the EXAFS contributions indicating $Pt-O_l$ (the subscript l refers to long) at a distance of 3.20 Å (with a coordination number of 3.4) and $Ru-O_l$ at a distance of 3.24 Å (with an average coordination number of 1.5). The fraction of the metal atoms in the clusters that are bonded to the surface is expected to depend on the degree of the support hydroxylation and the degree of nucleophilic attack of the hydroxyl groups on the metal-bound CO ligands.

High Dispersion of Decarbonylated Bimetallic Clusters. The EXAFS data (Tables 3 and 4) show that the average Pt−Pt and Ru−Ru coordination numbers characterizing the supported clusters formed by complete decarbonylation in He or H_2 at 300−400 °C were 2.0 and 4.0, respectively. These values are higher than those observed for the undecarbonylated γ-Al_2O_3-supported clusters represented as $[Pt_2Ru_4(CO)_{18}]$ (Table 1), consistent with the inference that some slight aggregation of the Pt and Ru took place upon decarbonylation.

The EXAFS data provide a basis for estimation of the degree of aggregation, as follows. As higher-shell structures were not evidenced by the EXAFS data, it follows from the coordination numbers N_{PtPt} and N_{RuRu} that the decarbonylated clusters incorporated no more than about three Pt and six Ru atoms each, on average, which *roughly* corresponds to aggregates of two Pt_2Ru_4 cluster units. The data indicate that the Ru shows a greater tendency for aggregation than the Pt, although both metals interact with the support, as indicated by the $Pt-O_{support}$ and $Ru-O_{support}$ contributions (Tables 3 and 4).

In summary, an important result, clearly demonstrated by the data, is that, in the temperature range of 300−400 °C, the degree of metal aggregation was extremely low, regardless of the atmosphere (He or H_2) used for decarbonylation of $[Pt_2Ru_4(CO)_{18}]$.

These data are in contrast to an earlier report indicating that the decarbonylation of the carbon-supported $[Pt_2Ru_4(CO)_{18}]$ in H_2 at 400 °C resulted in the formation of relatively large layer-segregated nanoparticles incorporating tens of Pt and Ru atoms.[6] We attribute the formation of the relatively large bimetallic structures to the relatively high mobility of Pt and Ru atoms (or other cluster fragments) on carbon; the cluster−support interactions on carbon are expected to be much weaker than those on γ-Al_2O_3. In support of this expectation, we cite literature[37] data indicating that the average size of Pd particles in Pd/C was doubled by increasing the temperature of H_2 treatment from 300 to 400 °C, whereas γ-Al_2O_3-supported Pt particles are resistant to sintering in this temperature range, even when a combination of O_2 and H_2 treatments is applied.[38] Furthermore, electron micrographs show that the migration of Pt atoms on carbon (graphite) surfaces in the presence of H_2 is accompanied by the formation of channels, consistent with the gasification of the carbon support catalyzed by Pt.[39]

Thus, the choice of the support and treatment conditions used to decarbonylate the γ-Al_2O_3-supported $[Pt_2Ru_4(CO)_{18}]$ are crucial in determining the dispersion of the resultant PtRu species. We know of no more highly dispersed supported bimetallics than ours that consist of platinum-group metals.

Structural Changes of the Metal Frame during Decarbonylation. The EXAFS data show that the decarbonylation of the supported $[Pt_2Ru_4(CO)_{18}]$ was accompanied by some structural rearrangement of the metal core of the clusters. Specifically, the data of Tables 3 and 4 show that after treatment in He or H_2 at 300−400 °C, the Pt−Pt and Ru−Ru bond distances were 2.69 and 2.64 Å, respectively. Thus, the Pt−Pt bond distance increased by 0.03 Å and the Ru−Ru bond distance decreased by 0.19 Å relative to the values characterizing the fully carbonylated cluster precursor in the crystalline form or supported on γ-Al_2O_3 (Table 1).

Similarly, decarbonylation in H_2 of $[PtRu_5C(CO)_{16}]$ and of $[Pt_2Ru_4(CO)_{18}]$, each supported on carbon, gave PtRu clusters characterized by shorter Pt−Pt and Ru−Ru bond distances than those determined for the respective crystalline precursors.[6,40,41] However, in contrast to our results, the decarbonylation of these metal carbonyl clusters was accompanied by the formation of layers of segregated nanoparticles incorporating about 40 Pt atoms and Ru atoms and having average diameters of about 15 Å; the structural change is associated with the aggregation and formation of alloy-like structures with the metal atoms being packed closer to each other than in the metal carbonyl precursors.[6,40,41]

Our data clearly show that even when our PtRu samples were highly dispersed, the Pt−Pt and Ru−Ru contributions characterizing the decarbonylated clusters were substantially different from those of the fully carbonylated species. Therefore, we doubt that the observed changes in the metal−metal bonds could be fully accounted for by just the aggregation. The EXAFS data reported for osmium subcarbonyls on γ-Al_2O_3 show that the

loss of one CO ligand during decarbonylation was accompanied by an increase in the $Os-O_{support}$ coordination number from nearly 3 to nearly 4, consistent with the suggestion that the lost CO ligand was replaced by an oxygen atom of the support.[42] We suggest that this conclusion can be extended to supported metal carbonyl clusters, so that the loss of a CO ligand could be compensated by metal−support interactions, with the support becoming part of the ligand shell of the (partially) decarbonylated species. Theoretical calculations[43] showing that the energy of the metal−$O_{support}$ bond is greater than that of the metal−CO bond for rhenium subcarbonyls supported on MgO and that the metal−support (metal−oxygen) interface bonds are strong[35,36] reinforce the view of the support as a ligand, which typically is multidentate. The theoretical simulations reported for SiO_2-supported $[Ru_{12}Cu_4C_2(CO)_{32}Cl_2]^{2-}$ show that the strong cluster−support interaction results in a structural modification of the cluster core upon removal of carbonyl ligands.[25] Theoretical predictions made for Os_5C clusters on MgO[44] and Ir_4 clusters on faujasite[35] indicate that removal of the CO ligands leads to contraction of the metal−metal bonds.

The experimental structure parameters determined from the EXAFS data for monometallic metal carbonyl clusters show, for example, that the Ir−Ir bond distance (2.68 Å) characterizing $[Ir_4(CO)_{12}]$, within the experimental uncertainty, remained the same after adsorption of the cluster on γ-Al_2O_3 and after subsequent decarbonylation.[45] On the other hand, the Rh−Rh bond distance was observed to shrink from 2.76 to 2.68 Å upon decarbonylation of NaY zeolite-supported $[Rh_6(CO)_{16}]$.[45] The greatest comparable decrease in metal−metal bond distance was observed upon decarbonylation of $[Ru_3(CO)_{12}]$ on various supports (MgO, SiO_2, TiO_2, and γ-Al_2O_3), whereby the Ru−Ru bond distance changed from approximately 2.88 to 2.64 Å.[45] The discrepancy between calculated and experimental EXAFS data observed for Ir clusters favors the suggestion that the supported Ir clusters characterized by EXAFS spectroscopy were not entirely ligand-free.[35] Although the computational results give a clear indication that the nature of the ligands as well as the strength of interaction between the metal core and the ligands can strongly affect the cluster morphology, we infer that the identities of the metals in the cluster core also need to be taken into consideration.

Strong Pt−Ru Interactions in Decarbonylated Clusters. The EXAFS data of Tables 3 and 4 show that regardless of the temperature or environment used to decarbonylate the supported $[Pt_2Ru_4(CO)_{18}]$, the Pt−Ru contributions remained, being detected at both the Pt L_{III} and Ru K edges in the decarbonylated samples. Nonetheless, the cluster frame of γ-Al_2O_3-supported $[Pt_2Ru_4(CO)_{18}]$ was found to undergo modifications upon decarbonylation—evidently, the Pt−Ru interactions in the original cluster frame were strong enough to survive these changes.

To be reliable and consistent, the fit of the EXAFS data must give parameters meeting some constraints: the parameters determined from each edge for the Pt−Ru interactions must indicate equivalent bond distances and Debye−Waller factors, with the coordination numbers N_{PtRu} and N_{RuPt} related to each other by the equation: $N_{PtRu}/N_{RuPt} = n_{Ru}/n_{Pt}$, where n_{Ru} and n_{Pt} are the total numbers of Ru and Pt atoms in the sample, respectively.[4,17,21] Good fits of the data were obtained when these constraints were applied. The EXAFS parameters (Tables 3 and 4) show that the average Pt−Ru distances and Debye−Waller factors determined from the Pt L_{III}-edge data match, within the expected uncertainties, those determined from the Ru K-edge data. The values of N_{PtRu}/N_{RuPt} determined from the data match the value of n_{Ru}/n_{Pt} of 2 calculated for these samples on the basis of the precursor stoichiometry. Moreover, the Pt−Ru bond distance of 2.68 Å observed for the decarbonylated samples agrees well with the value of 2.67 Å calculated as a sum of radii of the Pt−Pt and Ru−Ru contributions. Thus, the good agreement of structural parameters determined from both the Pt L_{III} and Ru K edges and characterizing the Pt−Ru interactions, with the constraints mentioned above, demonstrates the good internal consistency of the EXAFS data.

The observation that the Pt−Ru bond distance approximately satisfied the equation $R_{PtRu} = {}^1/_2(R_{PtPt} + R_{RuRu})$, where R_{PtPt} and R_{RuRu} are the bond distances characterizing the Pt−Pt and Ru−Ru contributions, respectively, suggests that another constraint is appropriate for bimetallic clusters consisting of two platinum-group metals. Thus, we recommend that an additional approximate constraint be that the distance between the two metals should with some generality approximately equal half the sum of the distances between the individual atoms of each metal.

Conclusions

IR and EXAFS spectroscopies were used to characterize the adsorption on γ-Al_2O_3 of molecular $[Pt_2Ru_4(CO)_{18}]$, a cluster in which the Pt and Ru atoms are bonded to each other. The data show that the majority of the bimetallic cluster precursor was only weakly adsorbed on the support, interacting by hydrogen bonding of its carbonyl ligands with surface hydroxyl groups of the support. The weakness of the cluster−support interactions allowed retention of the cluster frame in the supported cluster and recovery of the clusters from the surface by extraction with CH_2Cl_2. The data also indicate that a minority of the bimetallic clusters interacted strongly with the support, likely forming some partially decarbonylated surface species of unknown structure as a result of nucleophilic displacement of carbonyl ligands by surface hydroxyl groups. The carbonyl ligands of the supported clusters were removed by treatment in He or H_2 at 300−400 °C, and the resulting supported bimetallic species were characterized by EXAFS spectroscopy. Structural changes of the cluster core occurred upon decarbonylation, as indicated by changes in the Pt−Pt and Ru−Ru bond distances relative to those of the fully carbonylated clusters. Nevertheless, the bimetallic cluster frame remained intact after full decarbonylation, as evidenced by the presence of strong Pt−Ru contributions at both Pt L_{III} and Ru K edges. Average Pt−Pt and Ru−Ru coordination numbers characterizing the decarbonylated species were found to be 2.0 and 4.0, respectively, signifying extremely high dispersions of the resulting supported bimetallic species. The high dispersion is believed to be the result of strong interactions between Pt and Ru atoms, which limit the surface mobility of the metals.

Acknowledgment. This research was supported by Ford Motor Co. The EXAFS experiments were done at the Stanford Synchrotron Radiation Laboratory, a national user facility operated by Stanford University on behalf of the U.S. Department of Energy, Office of Basic Energy Sciences. The EXAFS data were analyzed with the XDAP software developed by Vaarkamp et al.[12]

References and Notes

(1) *Catalytic Naphtha Reforming*; Antos, G. A., Aitani, A. M., Parera, J. M., Eds.; Marcel Dekker: New York, 1995.

(2) Shelef, M.; Graham, G. W. *Catal. Rev.−Sci. Eng.* **1994**, *36*, 433.

(3) Braunstein, P.; Rosé, J. In *Catalysis by Di- and Polynuclear Metal Cluster Complexes*; Adams, R. D., Cotton, F. A., Eds.; Wiley-VCH: Weinheim, 1998; p 443.
(4) Alexeev, O. S.; Graham, G. W.; Shelef, M.; Gates, B. C. *J. Catal*. **2000**, *190*, 157.
(5) Ponec, V.; Bond, G. C. *Stud. Surf. Sci. Catal*. **1995**, *95*, 1.
(6) Hills, C. W.; Nasher, M. S.; Frenkel, A. I.; Shapley, J. R.; Nuzzo, R. G. *Langmuir* **1999**, *15*, 690.
(7) Alexeev, O.; Panjabi, G.; Gates, B. C. *J. Catal.* **1998**, *173*, 196.
(8) Adams, R. D.; Chen, G.; Wu, W. *J. Cluster Sci.* **1993**, *4*, 119.
(9) Alexeev, O.; Gates, B. C. *J. Catal.* **1998**, *176*, 310.
(10) Mojet, B. L.; Koningsberger, D. C. *Catal. Lett.* **1996**, *39*, 191.
(11) Rehr, J. J.; Mustre de Leon, J.; Zabinsky, S. I.; Albers, R. C. *J. Am. Chem. Soc.* **1991**, *113*, 5135.
(12) Vaarkamp, M.; Linders, J. C.; Koningsberger, D. C. *Physica B* **1995**, *208*−*209*, 159.
(13) Stern, E. A. *Phys. Rev. B* **1993**, *48*, 9825.
(14) Brigham, E. O. *The Fast Fourier Transform*; Prentice Hall: Englewood Cliffs, NJ, 1974.
(15) Kirlin, P. S.; van Zon, F. B. M.; Koningsberger, D. C.; Gates, B. C. *J. Phys. Chem.* **1990**, *94*, 8439.
(16) van Zon, J. B. A. D.; Koningsberger, D. C.; van't Blik, H. F. J.; Sayers, D. E. *J. Chem. Phys.* **1985**, *82*, 5742.
(17) Alexeev, O.; Shelef, M.; Gates, B. C. *J. Catal.* **1996**, *164*, 1.
(18) Koningsberger, D. C. In *Synchrotron Techniques in Interfacial Electrochemistry;* Melendres, C. A., Tadjeddine, A., Eds.; Kluwer: Dordrecht, 1994.
(19) Knözinger, H.; Ratnasamy, P. *Catal. Rev. Sci. Eng.* **1978**, *17*, 201.
(20) Kiselev, A. V. *Infrared Spectra of Surface Compounds;* Wiley: New York, 1975.
(21) Via, G. H.; Drake, K. F.; Meitzner, G.; Lytle, F. W.; Sinfelt, J. H. *Catal. Lett.* **1990**, *5*, 25.
(22) Braterman, P. S. *Metal Carbonyl Spectra*; Academic Press: London, 1975.
(23) Lamb, H. H.; Gates, B. C. *J. Am. Chem. Soc.*, **1986**, *108*, 81.
(24) Bromley, S. T.; Sankar, G.; Catlow, C. R. A.; Thomas, J. M.; Manschmeyer, T. *Microporous Mesoporous Mater.* **2001**, *44*−*45*, 395.
(25) Bromley, S. T.; Sankar, G.; Catlow, C. R. A.; Manschmeyer, T.; Johnson, B. F. G.; Thomas, J. M. *Chem. Phys. Lett.* **2001**, *340*, 524.
(26) Gates, B. C. In *Catalysis by Di- and Polynuclear Metal Cluster Complexes*; Adams, R. D., Cotton, F. A., Eds.; Wiley-VCH: Weinheim, 1998; p 509.
(27) Guczi, L.; Beck, A. *Polyhedron* **1988**, *7*, 2387.
(28) Bender, R.; Braunstein, P. *J. Chem. Soc., Chem. Commun.* **1983**, 334.
(29) Bergmeister, J. J.; Hanson, B. E. *Organometallics* **1989**, *8*, 283.
(30) Brown, T. L. *J. Mol. Catal.* **1981**, *12*, 41.
(31) Keyes, M. P.; Gron, L. U.; Watters, K. L. *Inorg. Chem.* **1989**, *28*, 1236.
(32) Myllyoja, S.; Suvanto, M.; Kurhinen, M.; Hirva, P.; Pakkanen, T. A. *Surf. Sci.* **1999**, *441*, 454.
(33) Ungermann, C.; Landis, V.; Moya, S. A.; Cohen, H.; Walker, H.; Pearson, R. G.; Rinker, R. G.; Ford, P. C. *J. Am. Chem. Soc.* **1979**, *101*, 5922.
(34) Koningsberger, D. C.; Gates, B. C. *Catal. Lett.* **1992**, *14*, 271.
(35) Ferrari, A. M.; Neyman, K. M.; Mayer, M.; Staufer, M.; Gates, B. C.; Rösch, N. *J. Phys. Chem. B* **1999**, *103*, 5311.
(36) Lopez, N.; Illas, F.; Pacchioni, G. *J. Phys. Chem. B* **1999**, *103*, 1712.
(37) Ryndin, Yu. A.; Alekseev, O. S.; Paukshtis, E. A.; Zaikovskii, V. I.; Kalinkin, A. V. *J. Mol. Catal.* **1991**, *68*, 355.
(38) Alexeev, O.; Kim, D.-W.; Graham, G. W.; Shelef, M.; Gates, B. C. *J. Catal.* **1999**, *185*, 170.
(39) Goethel, P. J.; Yang, R. T. *J. Catal.* **1988**, *108*, 356.
(40) Nashner, M. S.; Frenkel, A. I.; Adler, D. L.; Shapley, J. R.; Nuzzo, R. G. *J. Am. Chem. Soc.* **1997**, *119*, 7760.
(41) Nashner, M. S.; Frenkel, A. I.; Somerville, D.; Hills, C. W.; Shapley, J. R.; Nuzzo, R. G. *J. Am. Chem. Soc.* **1998**, *120*, 8093.
(42) Deutsch, S. E.; Chang, J.-R.; Gates, B. C. *Langmuir* **1993**, *9*, 1284.
(43) Hu, A.; Neyman, K. M.; Staufer, M.; Belling, T.; Gates, B. C.; Rösch, N. *J. Am. Chem. Soc.* **1999**, *121*, 4522.
(44) Goellner, J. F.; Neyman, K. M.; Mayer, M.; Nörtemann, F.; Gates, B. C.; Rösch, N. *Langmuir* **2000**, *16*, 2736.
(45) Alexeev, O.; Gates, B. C. *Top. Catal.* **2000**, *10*, 273.